

## Neutron Diffraction Studies on Iron at High Temperatures

M. K. WILKINSON AND C. G. SHULL\*

*Oak Ridge National Laboratory, Oak Ridge, Tennessee*

(Received April 26, 1956)

Neutron diffraction measurements have been made on iron at a series of elevated temperatures up to about 1000°C to establish the magnetic scattering effects through the Curie temperature and in the  $\gamma$ -phase region. Diffraction patterns obtained for the face-centered-cubic  $\gamma$  phase offer no evidence for an anti-ferromagnetic structure in  $\gamma$  iron at high temperatures, and the diffuse scattering above  $T_c$  suggests that both phases of the metallic lattice are paramagnetic in that temperature region. At temperatures up to the  $\alpha$ - $\gamma$  phase transformation, the paramagnetic scattering suggests the existence of considerable ferromagnetic short range order. Pronounced small-angle scattering was found to develop in the temperature region around the Curie transition, and this type of scattering is explained on the basis of the critical magnetic scattering suggested by Van Hove. Detailed investigations, which included experiments on nickel and magnetite near their Curie transitions, were performed to determine the general characteristics of the critical magnetic scattering.

### INTRODUCTION

IT is well known that the ferromagnetic elements of the iron group (iron, cobalt, and nickel) all exhibit magnetic properties at temperatures above their Curie transitions which are not easily correlated with their ferromagnetic properties. The variation of the inverse susceptibility with temperature in the paramagnetic region for these elements is not quite linear, and the assumption of a Curie-Weiss behavior suggests larger values for the atomic magnetic moments than those measured for the ferromagnetic state. Specifically for iron, in contrast to a ferromagnetic moment of 2.22 Bohr magnetons per atom, the temperature dependence of the susceptibility above the Curie temperature of 770°C suggests an atomic magnetic moment of about  $3.4\mu_B$  in the alpha-phase region and above  $10\mu_B$  in the higher temperature gamma phase. This anomalous behavior has been considered of sufficient significance that several theories of the ferromagnetic structure have been advanced which account for both the paramagnetic and ferromagnetic properties.

Previous reports have been given<sup>1,2</sup> on the magnetic scattering of neutrons by iron and cobalt in the ferromagnetic state, and the implication of these results on the ferromagnetic structure has been discussed. The present report<sup>3</sup> extends the neutron scattering observations into the high-temperature paramagnetic region for both the alpha and gamma phases of iron. During these investigations an intense small-angle scattering was found to exist in both the ferromagnetic and the paramagnetic states at sample temperatures near the Curie transition, and considerable study has been made of this scattering. Although the present report will deal primarily with studies on iron, some small-angle scattering data

have been obtained for nickel and magnetite, and these results will be included.

### EXPERIMENTAL TECHNIQUES

In order to study the scattering characteristics of iron at high temperatures, it was necessary to enclose the sample in a good vacuum to eliminate oxidation and sample disintegration. A vacuum furnace was constructed for this purpose with resistance heating attached directly to the ends of the sample block. The sample was Armco iron (spectroscopic purity 99.92%) which had been mechanically worked to produce small grain size. Originally an ingot of cylindrical shape about 6 inches long and 1 inch in diameter, the central region was machined into a flat-plate section of  $\frac{3}{8}$ -inch thickness through which the neutron radiation passed. Tantalum resistance wires were cemented to the two cylindrical ends of the ingot, and the central specimen temperature was established with a calibrated Pt, Pt-Rh thermocouple. The sample block was supported by thermal insulators with a devious path to the vacuum envelope. A chain of four floating radiation shields surrounded the specimen and these shields served to decrease very materially thermal radiation losses to the external vacuum shell. The neutron radiation passed through windows of thin vanadium foil in the vacuum jacket and radiation shields, which minimized the neutron scattering effects from the furnace because of the very low neutron coherent scattering cross section of vanadium.

The cross-sectional area of the neutron beam was about  $\frac{1}{2}$  inch by 1 inch, whereas the sample plate area was 1 inch by  $1\frac{1}{4}$  inches. An oversize sample was advantageous in that expansion effects at the various temperatures could be properly considered in the evaluation of data. Moreover, with the thickness of the specimen plate such that the neutron transmission was close to  $1/e$ , the intensity of scattered neutrons was essentially independent of expansion effects, and no correction for expansion was necessary. The actual

\* Now with Massachusetts Institute of Technology assigned to Brookhaven National Laboratory, Upton, Long Island, New York.

<sup>1</sup> Shull, Wollan, and Koehler, *Phys. Rev.* **84**, 912 (1951).

<sup>2</sup> C. G. Shull and M. K. Wilkinson, *Revs. Modern Phys.* **25**, 100 (1953).

<sup>3</sup> Preliminary reports have been given by the authors in *Phys. Rev.* **94**, 1439 (1954).

neutron transmission in the sample, of course, changed as the temperature of the sample was increased, and direct measurements of this effect were found to be in good agreement with calculated values using the known linear expansion coefficients of iron. Between 20°C and 700°C the observed transmission value increased by 2.1% whereas the calculated increase was evaluated as 2.0%.

With a power dissipation in this furnace of about 400 watts, a temperature of nearly 1000°C in the sample was obtainable at a pressure of about  $10^{-5}$  mm Hg. The diffraction patterns shown in Fig. 1 taken for iron at room temperature and at 971°C with a neutron wavelength of 0.90 Å are typical of those which were obtained. The low-temperature pattern is characteristic of the alpha or body-centered-cubic phase, while the high-temperature pattern shows the gamma or face-centered-cubic phase. The transformation from one phase to another can be studied easily by observing the diffracted intensities as a function of temperature. Figure 2 shows intensities which were measured at the angular position which corresponded to the (200) reflection in the  $\gamma$  phase. Data were obtained with the sample temperature both increasing and decreasing, and the temperature at the midpoint of the phase transformation on heating was determined to be 896°C. There is some variation in the published values for this transformation temperature, but for the purest samples, a midpoint-on-heating temperature of 910°C is frequently quoted. The slightly lower transformation temperature for our sample may have been caused by sample impurities or small errors in thermocouple calibration or measurement.

During the course of the high-temperature investigations on iron, it was found desirable to study some of the scattering characteristics with the sample in an external magnetic field while being maintained at elevated temperatures. A second vacuum furnace was constructed for this purpose which mounted around the pole pieces of an electromagnet such that the magnet

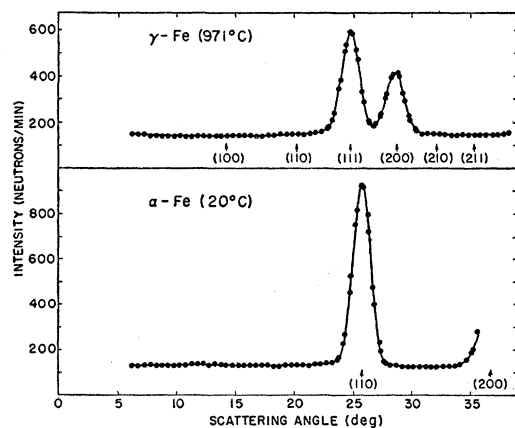


FIG. 1. Neutron diffraction patterns taken for polycrystalline iron in  $\alpha$  and  $\gamma$  phases.

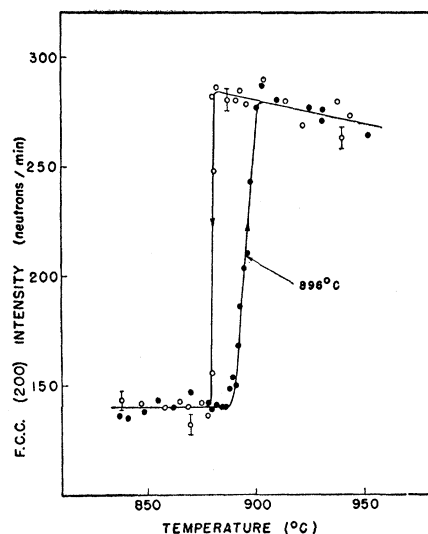


FIG. 2. Scattered neutron intensities showing  $\alpha$  to  $\gamma$  transformation in iron at high temperatures.

poles formed a part of the vacuum enclosure. The sample plate was supported by thermal insulators from one of the pole pieces and was heated by tantalum resistance windings which were attached in a fashion similar to those in the furnace just described. In order to prevent heating of the pole pieces, they were water-cooled through re-entrant ducts bored at positions which were not critical magnetically. Sample temperatures up to about 800°C were obtained in this furnace simultaneously with magnetization of the sample at an applied field strength of about 8000 oersteds.

## EXPERIMENTAL RESULTS

### Coherent Scattering from Iron

Figure 1 has illustrated the diffraction patterns obtained for iron in both the alpha and gamma phases. At temperatures lower than the Curie temperature for iron ( $T_c = 770^\circ\text{C}$ ), the coherent reflections of the alpha phase contain both nuclear and magnetic components with the latter decreasing in magnitude as  $T_c$  is approached. A qualitative indication of this temperature dependence is shown in Fig. 3 where the intensity of the (110) reflection is given for several temperatures. There is the usual decrease of the intensity with increasing temperature because of the increased lattice vibrations, and the magnitude of this effect is shown by the vectors at the different temperatures. An additional attenuation of the intensity is noted, and this decrease is a consequence of the elimination of the coherent ferromagnetic scattering as the Curie temperature was exceeded. The particular sample block used in obtaining the data of Fig. 3 was known to possess a small amount of preferred orientation of the small crystallites as established by measurements of the absolute intensity of scattering.

The quantitative determination of the ferromagnetic

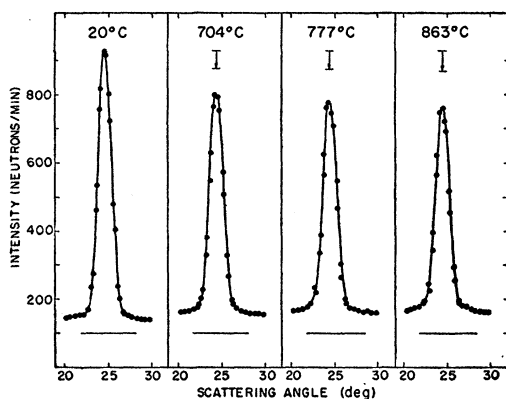


FIG. 3. Variation with temperature of the (110) reflection from  $\alpha$ -Fe. The vertical arrows represent the expected decrease in intensity due to lattice thermal effects.

intensity or cross section included in the reflections of Fig. 3 was carried out most significantly by magnetizing the sample during the scattering observations. If the atomic magnetic moments are oriented parallel to the scattering vector, the magnetic scattering amplitude falls to zero, and the intensity change upon magnetization can be used to evaluate the magnetic scattering cross section. A small correction for the altered magnetic transparency of the sample, the single-transmission effect, is necessary in this process. Figure 4 shows the magnetic intensity, expressed in absolute units of differential scattering cross section, in the (110) reflection from  $\alpha$ -iron as a function of sample temperature. The points represent experimental data and are to be compared with the calculated curve both on absolute scale and in temperature variation. The calculated cross sections are given by

$$p^2 = 0.1935 \times 10^{-24} S^2 f^2 (M_T/M_0)^2 \text{ cm}^2, \quad (1)$$

where  $S$  is the effective spin quantum number of the magnetic atoms (1.11 for iron),  $f$  is the magnetic amplitude form factor, and  $M_T/M_0$  is the magnetization at temperature  $T$  relative to that at absolute zero. For the (110) reflection a value of 0.590 for  $f$  was used which is the average of two theoretical calculations by Steinberger and Wick.<sup>4</sup> Satisfactory agreement between theory and experiment is indicated, although the sizeable uncertainty in the experimental data, arising principally because the nuclear scattering is about twelve times larger than the magnetic scattering, excludes a close comparison. However, the data are significant in showing that for this metallic lattice, as the Curie temperature is approached, the reduction in magnetization is accompanied by a loss of coherent scattering in a manner similar to that which occurs for ionic lattices. Moreover, it is seen that an applied field of about 8000 oersteds is effective in altering this coherent scattering at the various temperatures indicated.

<sup>4</sup> J. Steinberger and G. C. Wick, Phys. Rev. **76**, 994 (1949).

The neutron diffraction patterns taken for gamma-iron above the 900°C transformation as illustrated in Fig. 1 are characteristic of the face-centered-cubic lattice. Of interest is the fact that no magnetic superstructure lines are in evidence, since this implies that f.c.c. iron is not antiferromagnetic in its pure state at these temperatures. This observation is in disagreement with previous suggestions that  $\gamma$ -iron is antiferromagnetic,<sup>5,6</sup> although of course the present data are restricted to high temperatures.

### General Diffuse Scattering from Iron

In the present investigation, special attention has been placed on details of the diffuse scattering within the neutron diffraction patterns and to the search for paramagnetic scattering above  $T_c$  from both alpha and gamma iron. When data at different temperatures are compared, it is necessary to correct for normal lattice temperature effects before the changes in magnetic scattering can be established. The Debye theory of independent oscillators has been found to describe quite well the temperature dependence of diffuse scattering in several nonmagnetic lattices, and this procedure has been used in correcting the high-temperature iron patterns. In the calculations for sample temperatures in the alpha phase, a Debye characteristic temperature of 453°K was used. It has been suggested recently<sup>7</sup> that the Debye  $\Theta$  changes at the phase transformation and that a value of 335°K is representative of the gamma phase. This value has been used in correcting the intensities in the gamma-Fe patterns. Lattice expansion effects can be quite sizeable over the wide temperature range encountered in these investigations, but fortunately this problem could be eliminated by proper specimen geometry and thickness.

A noticeable change with temperature in the diffuse level around the feet of the (110) reflection has been illustrated in Fig. 3. In Fig. 5 the general diffuse scattering is shown at angles smaller than that for the first coherent reflection. The observed diffuse scattering has been corrected for instrumental scattering (arising from the collimating system, vacuum and thermal

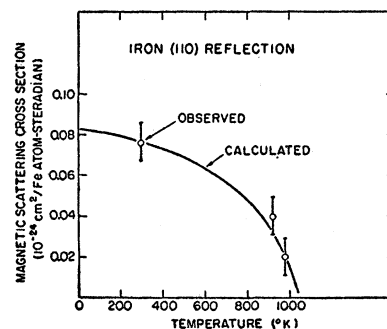


FIG. 4. Magnetic scattering cross section in the (110) reflection of  $\alpha$ -Fe as a function of temperature.

<sup>5</sup> R. Forrer, Ann. phys. **7**, Series 12, 605 (1952).

<sup>6</sup> F. Bader, Z. Naturforsch. **8a**, 675 (1953).

<sup>7</sup> R. J. Weiss and K. J. Tauer, Phys. Rev. **102**, 1490 (1956).

radiation shields, and general counter background), and for each temperature the appropriate correction for thermal diffuse scattering calculated by the Debye theory has been applied. Thus, the illustrated change in the experimental diffuse level with temperature is indicative of increased magnetic disorder scattering caused by the increased misalignment of the atomic magnetic moments within the magnetic lattice.

At temperatures in the ferromagnetic region below  $T_c$ , disorder scattering was found to be present as illustrated by the 689°C curve, and further increase in this diffuse level was seen as the sample became paramagnetic, with a marked change occurring at small angles. For comparison purposes, a curve showing the expected diffuse-scattering level in the paramagnetic region has been included on the figure. This curve was obtained by adding the calculated paramagnetic scattering to the diffuse level determined experimentally at 20°C. It is perhaps of interest to describe briefly the method used in this calculation before discussing the significance of the observed scattering levels.

Halpern and Johnson<sup>8</sup> have calculated the neutron differential scattering cross section of a paramagnetic atom or ion which is without coupling to any neighbors to be

$$d\sigma_{\text{para}} = \frac{2}{3}S(S+1)(e^2\gamma/mc^2)^2 f^2 d\Omega, \quad (2)$$

where  $S$  is the spin quantum number of the scattering atom,  $f$  the magnetic amplitude form factor,  $\gamma$  the neutron magnetic moment in nuclear Bohr magnetons, and the other terms have their conventional significance. This expression can be considered the sum of two components, one proportional to  $S^2$  and the other proportional to  $S$ . The  $S^2$  term is of an elastic scattering nature and originates from a scattering process which leaves the orientation of an individual spin unchanged with respect to that of its neighbors. The type of scattering which arises from this scattering interaction is either diffuse or coherent depending on the periodicity of the directions of the atomic magnetic moments within the lattice. When a material is examined at temperatures very low compared to its Néel or Curie transition and the magnetic lattice is ordered, there are diffraction peaks with intensities proportional to  $S^2$ , but when the

temperature of the sample is raised much higher than its magnetic ordering temperature, this scattering is transformed into diffuse scattering which is the  $S^2$  term of the above equation. On the other hand, the  $S$  term in Eq. (2) represents the "spin-flip" cross section which arises when the orientation of an individual atomic moment is changed. When the moment is flipped against the exchange or coupling energy associated with its neighbors, this process can alter the kinetic energy of the neutron which is scattered,<sup>9</sup> and is therefore inelastic.

For scattering from a particular specimen, the actual cross section associated with the spin-flip process will depend in a complicated manner upon the exchange energy (or  $T_c$ ) relative to the energy of the incident neutrons. In first approximation, however, the presence of the  $S$  term in Eq. (2) is not dependent on the sample temperature. This approximation appears quite valid for conditions where the coupling energy between spins is much lower than the neutron energy. It is less valid for cases where the neutron energy is lower than the coupling energy or where the two energy values are comparable. In these latter cases, it is possible that the amount of the "spin-flip" term will vary with sample temperature, since the coupling energy of the spins may be temperature sensitive. However, within the validity of this approximation, when the sample temperature is changed from a value much lower than  $T_c$  to one well into the paramagnetic region, a change in diffuse scattering given by the  $S^2$  term in Eq. (2) is to be expected.

This assumption is not completely valid in the present case of iron, but for the temperature range of the experimental data, it is unlikely that the contribution from the "spin-flip" term changes appreciably. Hence, this calculation has been made for iron with the effective spin quantum number of 1.11 which corresponds to the ferromagnetic moment. The calculated curve in Fig. 5 is the sum of the  $S^2$  term of Eq. (2) and the experimental data taken at room temperature. Except at small angles, the data observed at temperatures in the paramagnetic region do not attain this paramagnetic level, but inside 4 or 5 degrees scattering angle, the paramagnetic level is reached and exceeded. This characteristic in the angular distribution agrees with that expected if *ferromagnetic* short-range order were present. For the present data such an angular variation is quite reasonable since the highest temperatures attainable were only about 200°C above  $T_c$ , and considerable short-range order might be expected in the patterns at these temperatures. Weiss<sup>10</sup> has given a theoretical discussion of short-range-order effects in iron above  $T_c$  and has demonstrated their influence on the paramagnetic

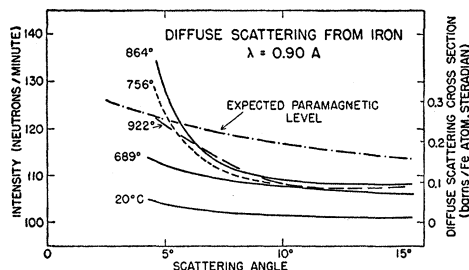


Fig. 5. Diffuse scattering in neutron diffraction patterns for iron at different temperatures.

<sup>8</sup> O. Halpern and M. H. Johnson, Phys. Rev. **55**, 898 (1939).

<sup>9</sup> This concept was implied in reference 8 and has been developed by S. Tamor and G. T. Trammell in unpublished treatments. See also R. A. Erickson, Phys. Rev. **90**, 779 (1953).

<sup>10</sup> P. R. Weiss, Phys. Rev. **74**, 1493 (1948).

susceptibility. Slotnick<sup>11</sup> has pointed out that ferromagnetic short-range order should give enhanced paramagnetic scattering at small angles (at the expense of the scattering in other regions) whereas antiferromagnetic short-range order should show an attenuation of the paramagnetic scattering at small angles as has been shown experimentally.<sup>12</sup>

Thus the diffuse-scattering curves demonstrate that there is magnetic scattering produced above  $T_c$  and hence that definite atomic magnetic moments are in existence in the paramagnetic region. Moreover, aside from the violent intensity variations noticed in the small-angle region, the general diffuse-scattering level appears little changed in the alpha to gamma transformation and hence equivalent atomic magnetic moments are suggested in the two phases. This conclusion is in disagreement with those from a study of the f.c.c. Fe-Mn system by Weiss, Corliss, and Hastings<sup>13</sup> in which a weak antiferromagnetism with low Néel temperature is suggested for pure f.c.c. Fe by extrapolation of the alloy properties. It is not clear how these two experiments are to be reconciled with each other.

It is difficult to assign a paramagnetic moment from the scattering data because of the short-range order which was present. However, in the absence of a detailed short-range-order calculation, it is thought that the data support the calculated paramagnetic scattering to within perhaps 50% in cross section. This, in turn, implies that the value of the paramagnetic moment in both the alpha and gamma iron is within 25% of the ferromagnetic moment. As mentioned previously, high-temperature susceptibility data for iron have suggested quite large moments in the paramagnetic state, and these larger moments appear to be beyond the range suggested by the scattering observations.

### Small-Angle Scattering from Iron

#### General Characteristics

The diffuse-scattering curves in Fig. 5 show the development of an intense small-angle scattering at temperatures in the vicinity of  $T_c$ , and a concentrated study has been made of this scattering. In order to obtain data at the small angles required, it was necessary to refine the collimating and detecting slit systems, and a pair of Soller slits of adjustable angular opening was used to permit study into scattering angles of about one degree. Figure 6 represents small-angle scattering data at various temperatures into the  $\gamma$ -phase region. The intensity which is plotted is that in excess of the intensity at 20°C. Therefore, the curves represent the additional magnetic intensity at each temperature, since no lattice thermal scattering is to be expected in this angular region. It is seen that the scattering rises

to a maximum in the vicinity of  $T_c$  and then falls rapidly as the sample becomes paramagnetic. Moreover, it is seen that the angular distribution of the scattering changes with temperature, and some of the curves actually cross others.

Since these angular distribution curves were obtained with slit geometry to get maximum scattered intensity, it was necessary to apply suitable slit corrections to the data before the absolute scattering cross sections could be evaluated. This correction procedure alters the shape of the angular distributions, and analysis shows that the true scattering distributions are even more strongly angle-dependent than those which were experimentally observed. As an indication of the cross-section scale associated with the intensities in Fig. 6, the differential scattering cross section at 754°C corresponding to a scattering angle of 1° and an effective neutron wavelength of 0.90 Å was evaluated as  $26 \times 10^{-24}$  cm<sup>2</sup> per iron atom. This value is very much larger than the calculated paramagnetic cross section shown in Fig. 5.

Some hysteresis effects which depended upon the thermal history of the specimen were noted in the small-angle scattering distributions. Small variations were found depending on whether the specimen temperatures were increased from the ferromagnetic state or reduced from the paramagnetic state, and particularly whether they were reduced from the  $\gamma$ -phase region. These effects were not too pronounced, however, and the curves shown in Fig. 6 are representative of the scatter-

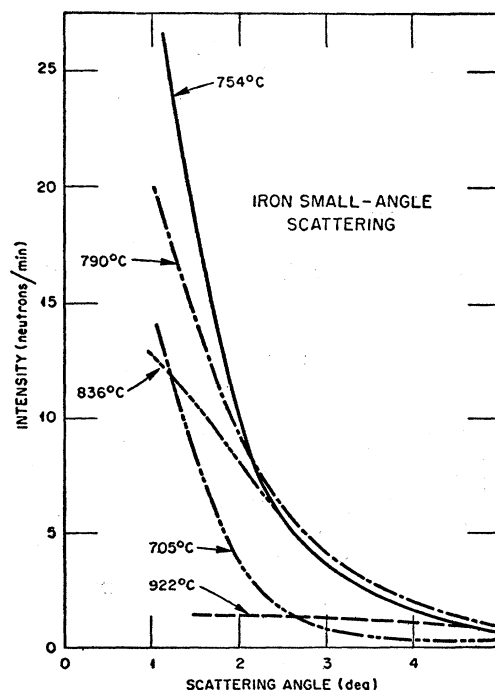


FIG. 6. Small-angle scattering produced by iron at different temperatures. The intensity shown is that in excess of the room temperature intensity.

<sup>11</sup> M. Slotnick, Phys. Rev. **83**, 1226 (1951).

<sup>12</sup> Shull, Strauser, and Wollan, Phys. Rev. **83**, 333 (1951).

<sup>13</sup> Weiss, Corliss, and Hastings (private communication).

ing which was obtained when the temperature of the sample was increased to each value.

Further details of the development of small-angle scattering with temperature are shown in Fig. 7. With the detector set at a fixed scattering angle of 1 degree and 1.218 Å neutrons incident on a polycrystalline iron ingot, the intensity of scattering was studied as the specimen temperature was varied. A pronounced increase in intensity is seen to occur at temperatures in the 500°C region and this intensity reaches a maximum at a temperature close to  $T_c$ . Above  $T_c$  the intensity decreases in a manner more or less symmetrical with the data below  $T_c$  until the  $\alpha$ - $\gamma$  transformation occurs. At the temperature of the phase transformation, there is a sudden drop in the residual scattering to a level which is essentially constant up to the highest temperature which was studied. This discontinuity in the scattering at an angle of one degree has been studied a number of times with different samples, and it exhibits the usual temperature hysteresis found in the  $\alpha$ - $\gamma$  transformation. Figure 7 also includes a cross-section scale which again indicates the strength of this scattering relative to the much smaller paramagnetic scattering.

When measurements were made in this manner at a fixed angle with different temperatures, it was found that the low-temperature intensity was not reproducible but increased with continued high-temperature exposure of the specimen. This is indicated in Fig. 7 by the room-temperature intensity at the start of the experiment (the circled point) compared to the final cooling curve which showed a significant increase over this level. It was established that this shift in the scattered intensity was not caused by changing conditions of the radiation shields and windows in the furnace. Furthermore, different samples of iron showed this effect in different degrees. It was more pronounced in those samples which had experienced the most extensive thermal cycling history, and any one sample would show increased effects upon continued heating to high temperatures. On the other hand, the peak cross section at  $T_c$  showed no significant changes with the thermal history of the sample.

The origin of this variable background scattering is not understood. A possible explanation for its presence could result if there were a temperature dependence in the refractive-index type of magnetic scattering found by Hughes, Burgy, Heller, and Wallace.<sup>14</sup> This scattering arises because differently oriented domains exhibit different refractive indices to a neutron beam, thereby causing a broadening of the beam. Thus, if the domain structures in the present scattering samples were changing with heat treatment, the scattered radiation passing through the Soller slit system of the detector would be altered.

The appearance of the pronounced maximum in the

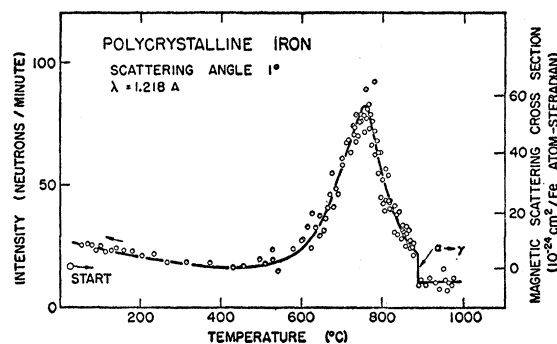


FIG. 7. Temperature variation of the scattered intensity from polycrystalline iron at a fixed detector angle of 1°. Pronounced critical scattering is noted around the Curie temperature.

small-angle scattering suggests that it arises from small clusters of aligned magnetic moments in the lattice which have a spatial extent that is temperature-dependent. Van Hove<sup>15,16</sup> has recently treated the case of neutron scattering by systems of interacting particles with particular emphasis on transition regions such as liquids and dense gases near the critical point and ferromagnetic materials near the Curie point. His theory predicts the development of a pronounced magnetic scattering at temperatures near a Curie transition which he has termed "critical magnetic scattering." This type of scattering is the result of spontaneous fluctuations in the magnetic moment density which increase in magnitude as the Curie point is approached and become very large at temperatures near  $T_c$ . The observed small-angle scattering is undoubtedly associated with Van Hove's critical scattering, but before discussing its implications, additional observational data will be presented.

#### *Dependence of Small-Angle Scattering on an External Magnetic Field*

As mentioned in an earlier section, the intensity of ferromagnetic coherent scattering is usually sensitive to the application of an external magnetic field to the scattering specimen. This change in the scattered intensity results because a magnetic field of sufficient intensity will align the direction of magnetization of the magnetic domains along the field direction, and the magnetic scattering of neutrons depends on the relative orientation of the atomic magnetic moments with respect to the scattering vector. In particular, if the moments are parallel to the scattering vector, the magnetic scattering amplitude becomes zero, and no coherent magnetic scattering is present. It was of interest to examine the sensitivity of the observed small-angle scattering to the application of an external magnetic field.

In this type of experiment, it was obviously necessary

<sup>14</sup> Hughes, Burgy, Heller, and Wallace, Phys. Rev. **75**, 565 (1949).

<sup>15</sup> L. Van Hove, Phys. Rev. **95**, 249 (1954).

<sup>16</sup> L. Van Hove, Phys. Rev. **95**, 1374 (1954).

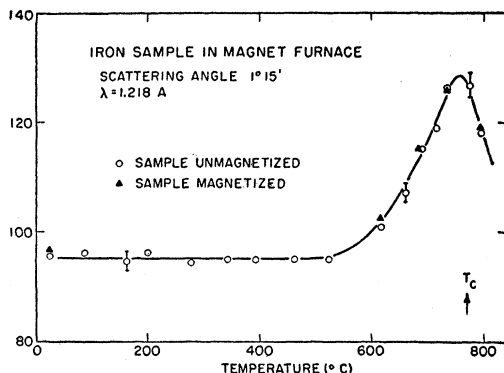


FIG. 8. Effect of an external magnetic field on the small-angle scattering produced by iron. In the magnetized samples the magnetization vector was aligned parallel to the scattering vector.

to define the external field direction relative to the scattering vector associated with the small-angle scattering. Hence, the usual Soller slit system could not be used because of the very large vertical divergence of the neutron beam within the slit openings relative to the small horizontal scattering angle. This difficulty was surmounted by constructing a Soller slit system in the incident and scattered beams which limited both the vertical and horizontal divergence. In practice, these slits were constructed by stacking thin cadmium sheets which had been folded with V-shaped grooves. The neutron beam through these slits was passed through an iron sample contained in a high-vacuum enclosure within the gap of an electromagnet as described in a previous section. Temperatures up to 800°C were attainable with an applied field strength of about 8000 oersteds.

Figure 8 shows the development of the scattered intensity at an angle of 1°15' as the temperature was increased through  $T_c$ . Data are shown both for the sample unmagnetized and magnetized parallel to the scattering vector. It is seen that there is no variation of this scattering with an external magnetic field of 8000 oersteds. Thus, the small-angle scattering is the same irrespective of whether the specimen is in a single-domain state or is of random polydomain nature.

#### Energy Changes in the Scattering Process

To determine whether the observed small-angle scattering was elastic or inelastic, some neutron-filter measurements of the scattered neutrons were made with a samarium filter consisting of a thin plate of  $\text{Sm}_2\text{O}_3$ . Samarium has a neutron capture cross section peaked at a neutron energy of 0.100 eV or a wavelength of 0.90 Å. Hence, such a filter can be used to determine if there is either an increase or decrease of wavelength when 0.90 Å neutrons are scattered by a sample. The transmission of the filter was studied both in the scattered beam at small angles and in the incident primary beam. From a comparison of these two transmission cross

sections, it was established that the wavelength of the scattered neutrons did not change by more than 5%. Thus, the small-angle scattering for this neutron energy appears to be closely elastic, since a wavelength change of less than 5% means a neutron energy change of less than 10% or 0.010 eV. Therefore, although the incident neutron energy was slightly larger than the exchange energy in iron, for which  $kT_c$  is about 0.090 eV, there were no significant energy changes in the scattering process.

#### Dependence of Small-Angle Scattering on Crystalline Structure

The small-angle scattering from a single crystal of pure iron (grown by the strain-anneal technique) has been studied for comparison with that produced by a polycrystalline sample. Figure 9 shows the increase in the scattered intensity of 1.218 Å neutrons measured at a fixed scattering angle of 1 degree when  $T_c$  was approached. For convenient comparison purposes, these data were obtained for a single crystal ingot of exactly the same dimensions as the polycrystalline sample used to obtain the data of Fig. 7, and identical observational conditions were used in the two experiments. Therefore, the intensity scales are directly comparable, and it is seen that the single-crystal results are the same as the polycrystalline results with respect to the development of scattering near the Curie temperature. Hence, this type of small-angle scattering is completely independent of the size and orientation of the crystalline grains in the iron specimen.

#### Small-Angle Scattering from Nickel

A sample of electrolytically-pure nickel has also been investigated at temperatures through its Curie transition (360°C) in a search for small-angle scattering, and Fig. 10 shows the results which were obtained. The lower curve indicates the scattered intensity as a function of temperature for the detector at a fixed angle of one degree, while the top curve shows the angular variation of the small-angle magnetic scattering for a temperature

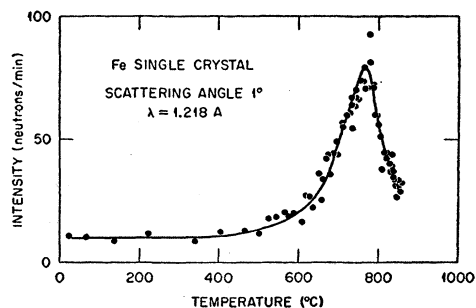


FIG. 9. Temperature variation of the small-angle scattering produced by a single crystal of iron. Specimen and beam characteristics were identical to those for the polycrystalline sample represented by the data in Fig. 7.

close to  $T_c$ . The latter curve represents the difference in the scattered intensity at 366°C relative to that at room temperature. An absolute cross-section scale is shown on the lower figure, and the critical scattering is seen to be very much smaller for nickel than that which was observed from iron. This difference would be expected since the values for the atomic magnetic moments present in nickel ( $0.61\mu_B$  as determined from ferromagnetic measurements) are considerably smaller than those in iron.

### Small-Angle Scattering from Magnetite

Magnetite ( $\text{Fe}_3\text{O}_4$ ) is a ferrimagnetic type of material in which the three iron atoms per molecule possess magnetic moments of +5, +4, and -5 Bohr magnetons. Although the individual atomic moments are large, the net ferromagnetic moment is much smaller ( $\frac{4}{3}\mu_B$  per iron atom) because of the antiparallel orientation of the moments. The development of additional small-angle scattering near the Curie temperature is shown in Fig. 11, where data are given for the scattering of 1.218 Å neutrons at a fixed angle of  $1^\circ$ . The absolute cross sections associated with this scattering are seen to be quite small. The small intensity of this scattering indicates that the net ferromagnetic moment determines the strength of the critical scattering rather than the values of the individual moments and suggests that the molecular group retains the internal orientation of its atomic moments in passing through the Curie temperature.

### DISCUSSION OF THE CRITICAL SCATTERING OBSERVATIONS

Perhaps the simplest explanation of the appearance of the critical magnetic scattering at small angles is obtained by a comparison with x-ray and light scattering phenomena. A highly collimated x-ray beam will be broadened upon passage through a colloidal substance because there exists a variation of scattering density from one region to another. The angular extent of this

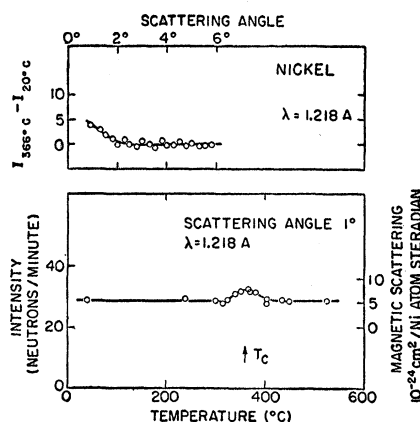


FIG. 10. Small-angle scattering obtained from nickel. The cross section associated with the critical scattering is seen to be very much smaller than that obtained for iron.

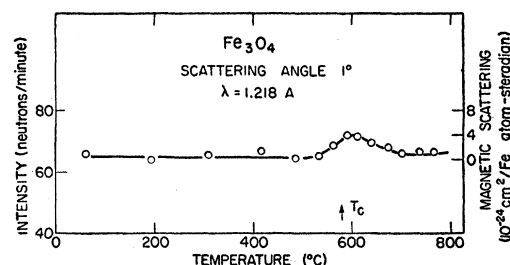


FIG. 11. Small-angle scattering obtained from magnetite ( $\text{Fe}_3\text{O}_4$ ).

broadening will depend inversely upon the ratio of the colloidal particle size and the radiation wavelength. By analogy, the critical magnetic scattering occurring at small angles can be pictured as arising from the presence of very large fluctuations in the magnetic scattering density within the sample at temperatures near  $T_c$ . An instantaneous picture of the magnetic lattice would show subregions within which an effective magnetization direction is defined, but this direction is different from one region to another, and these regions exhibit different magnetic scattering density to the incident neutrons. Since these magnetic fluctuations arise from thermal effects, they must be of dynamic nature with the instantaneous picture changing rapidly<sup>17</sup> with time. The fact that the critical scattering is insensitive to the bulk magnetization of the sample as affected by an applied magnetic field shows that the scattering does not result from a mere disruption in size of the static domain regions.

Figure 12 illustrates schematically this picture of fluctuations in the magnetic lattice. Far below the Curie transition, the magnetic moments within a domain are aligned parallel with only an occasional moment oriented in a different direction. At temperatures just below  $T_c$ , there still remains an effective domain magnetization both in magnitude and direction, but within the domain there exist fluctuation regions changing rapidly with time, which are responsible for the development of the critical scattering. The average size of these fluctuation regions reaches a maximum at  $T_c$ , and as the temperature is further increased, the regions become smaller. At temperatures significantly higher than  $T_c$ , the small regions with correlated spins are more commonly referred to as regions of short-range magnetic order. This local magnetic order exists until temperatures are reached far greater than  $T_c$  where the directions of the magnetic moments are independent of their neighbors.

An estimate of the size of the fluctuation regions can be obtained by applying small-angle scattering theory<sup>18</sup>

<sup>17</sup> From Eq. (AII.11) of reference 19, it is seen that the relaxation time of the magnetic fluctuations depends on the temperature and becomes longer as  $T_c$  is approached. At temperatures about 20 degrees from  $T_c$ , rough calculations predict the relaxation time to be about  $10^{-8}$  sec.

<sup>18</sup> For a general discussion see H. P. Klug and L. E. Alexander, *X-ray Diffraction Procedures* (John Wiley and Sons, Inc., New York, 1954), Chap. XII.



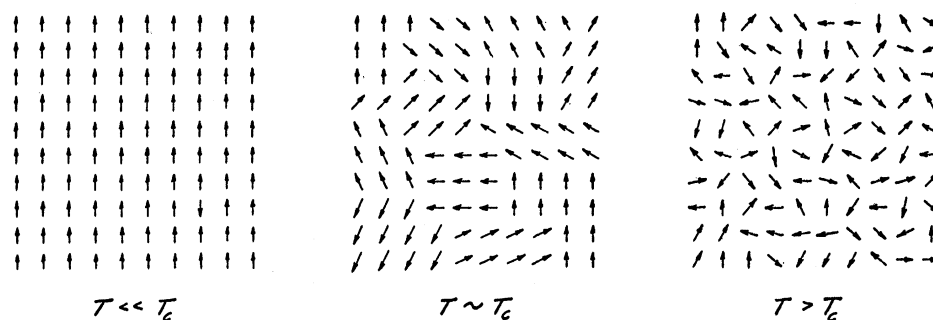


FIG. 12. Schematic diagram of the spin-correlation regions in a coupled magnetic lattice. The regions are of dynamic nature and must be considered to move continuously through the lattice.

to the angular distribution data as shown in Fig. 6. In this manner the angular distribution of the 754°C curve (just below  $T_c$ ) can be accounted for on the basis of a distribution of sizes ranging roughly between 12 Å and 25 Å, and relative to this range, the mean size of the fluctuation regions for the higher temperature curves would be smaller. Therefore, in the vicinity of  $T_c$  the magnetic spins are correlated out to considerable distances, and the range of this correlation gets smaller as the temperature is increased. The discontinuity in the critical scattering at the transformation from  $\alpha$ -Fe to  $\gamma$ -Fe suggests that a pronounced change occurs in this correlation when the lattice becomes face centered cubic.

Van Hove<sup>16</sup> has recently given a comprehensive treatment of the neutron scattering effects expected from a magnetic lattice in the vicinity of the Curie transition. His theory based on time-dependent spin correlations in ferromagnetic lattices predicts the development of a critical magnetic scattering near  $T_c$  which has the general features of the small-angle scattering observed in these experiments. A detailed analysis of the present data in terms of the Van Hove treatment has been performed, and this analysis will be discussed in a companion paper.<sup>19</sup>

<sup>19</sup> Gersch, Shull, and Wilkinson, Phys. Rev. **103**, 525 (1956), following paper.

The appearance of critical scattering near Curie transitions has been found and studied in other neutron scattering experiments. In studies of the transmission of long-wavelength neutrons through iron at high temperatures, Palevsky and Hughes<sup>20</sup> have found an anomalous increase in the transmission cross section near  $T_c$ . In similar experiments, Squires<sup>21</sup> found a large increase in the total cross section of iron and a much smaller increase in the total cross section of nickel near their respective ordering temperatures. McReynolds and Riste<sup>22</sup> have investigated the neutron scattering from a single crystal of magnetite, and in the vicinity of the Curie point they observed an abrupt increase in the diffuse intensity located near the (111) magnetic reflection. Undoubtedly, the origin of the small-angle scattering which we have observed from iron, nickel, and magnetite is closely related to that which produced the increased scattering in these other experiments.

#### ACKNOWLEDGMENTS

The authors wish to express their appreciation to H. Steiner and S. Mosko for help in performing the experiments and to H. A. Gersch and G. T. Trammell for very valuable discussions concerning the interpretation of the results.

<sup>20</sup> H. Palevsky and D. J. Hughes, Phys. Rev. **92**, 202 (1953).

<sup>21</sup> G. L. Squires, Proc. Phys. Soc. (London) **A67**, 248 (1954).

<sup>22</sup> A. W. McReynolds and T. Riste, Phys. Rev. **95**, 1161 (1954).